dicular to each others, whereas under the present experimental conditions the special pair has the Shipman-Katz geometry.

Acknowledgment. We thank P. A. Jager for technical assistance and Dr. G. Jansen and Dr. A. J. Hoff for valuable discussions of this work. We are indebted to Dr. J. Norris for a generous gift of perdeuterated chlorophyll and to Bruker AG, Zürich, for making available their NMR spectrometer for deuterium measurements. This work was supported by the Netherlands Foundation for Chemical Research (S.O.N.) with financial aid from the Netherlands Organization for the Advancement of Pure Research (Z.W.O.).

Registry No. (Chl a)$_2$, 18025-08-6.

Paramagnetic Carbon-13 Shifts Induced by the Free Radical Tempo. 2. Nitrogen Heterocycles

Zu Wen Qui,† David M. Grant,* and Ronald J. Pugmire

Contribution from the Department of Chemistry, University of Utah, Salt Lake City, Utah 84112. *Received July 12, 1982*

Abstract: With use of the free radical Tempo as a shift and relaxation reagent, both paramagnetic shifts and spin-lattice relaxation rates of nitrogen heterocycles are reported. Paramagnetic shifts of these compounds are larger than the corresponding shifts of the aromatic hydrocarbons, indicating a stronger interaction between nitrogen heterocyclic compounds and Tempo. Paramagnetic shifts increase with the number of nitrogen atoms per molecule. For pyridine type compounds, both shift and relaxation data show that the stronger interaction is not at the adjacent positions to the nitrogen atoms. It would appear in these heterocyclic complexes with Tempo that the nitrogen atoms tend to orient away from the N-O group in Tempo. In contrast, imidazole and indole exhibit a much stronger interaction with the Tempo due to hydrogen bond formation, and the positions near the N-H group exhibit larger paramagnetic shifts and relaxation rates. An approximate static model involving an indole-Tempo, hydrogen-bond complex accounts for the relaxation data from which both an equilibrium constant of complexation and a hydrogen-bond distance in the indole-Tempo complex could be estimated.

The relatively stable free radical Tempo has been used[1] in both aromatic and paraffinic hydrocarbons to induce paramagnetic shifts. The greater effectiveness of Tempo as a shift reagent compared with other free radicals was exhibited especially for the aromatic hydrocarbons. As a natural extension, induced spin-lattice relaxation rates along with paramagnetic shifts of ^{13}C in some nitrogen heterocycles are reported in this work. Nitrogen heterocycles are important compounds not only because of their structural similarity with aromatic hydrocarbons but also because of their intermolecular complexation capacity. Nitrogen heterocycles are also significant in the areas of biomedicine[2] and fossil fuels.[3]

The paramagnetic induced shift $\overline{\Delta\delta}_f$, in liquids results[4] from a contact interaction, $\overline{\Delta\delta}_f^{cont}$, and a dipolar interaction, $\overline{\Delta\delta}_f^{dip}$. The direct dipolar interaction between a magnetic moment of an unpaired electron, e, and a magnetic nucleus, N, is inversely proportional to r_{eN}^3, the distance between the free electron and the magnetic nucleus. The theoretical treatment of the pseudocontact term depends, among other things, on the anisotropy of the electron spin **g** tensor.[5] Hirayama and Honyu have assumed an axially symmetric **g** tensor in their treatment of Eu and Pr complexes in arriving at relative geometric factors for quinoline, isoquinoline, and acridine.[6] On the other hand, contact interactions arise from a finite unpaired electron spin density in s-type atomic orbitals centered on the nucleus. While the contact interaction is not explicitly distance dependent, it does depend upon the nature of the free radical and its proximity to the affected compound. Direct overlap of a molecular orbital containing the unpaired electron or induced unpaired spin density at the magnetic nucleus via a spin polarization mechanism is required to give an induced shift. Thus, the relative magnitude of these induced shifts at different nuclei within a molecule provide information on the average relative position of the Tempo with respect to the molecule. A quantitative description can only be obtained from an appropriate quantum mechanical calculation if the details of the intermolecular associations are known.

Levy and Komoroski[7] have shown that spin-lattice relaxation data complement paramagnetic shift data. At low concentrations of Tempo the induced shifts and line broadening are relatively small while effects upon the spin-lattice relaxation times (T_1's) are pronounced. The observed relaxation rate, R_1^{obsd}, the inverse of the T_1^{obsd}, is the sum of the various diamagnetic relaxation rates, R_1^{dia}, resulting from dipolar, spin-rotation, scalar, and chemical shift anisotropy mechanisms and from the paramagnetic relaxation rate R_1^e, due to the electron-nuclear relaxation mechanism. When the electron-nuclear dipole-dipole interaction dominates R_1^e, the usual sixth power distance dependence will control the relaxation, and the geometrical relationship between the free radical and the nitrogen heterocycle can be determined. Levy and Komoroski[7] successfully studied the interaction of isoborneol and phenol with $Cr(acac)_2$ and $Fe(acac)_3$. In this study of the indole-Tempo complex, the equilibrium constant and the average distance be-

† On leave from Jilin University, Changchun, Jilin, People's Republic of China.

(1) Qui, Z. W.; Grant, D. M.; Pugmire, R. J. *J. Am. Chem. Soc.* **1982**, *104*, 2747.

(2) Dwek, R. A.; Campbell, I. D.; Richards, R. E. "NMR in Biology"; Academic Press: New York, 1977.

(3) For coal the nitrogen content is usually in the 1-2% range on a moisture- and ash-free basis. Elliott, M. A., Ed. "Chemistry of Coal Utilization"; Wiley-Interscience: New York, 1981; p 28. For crude shale oil the nitrogen content is approximately the same. See, for instance: Fenton, D. M.; Henning, H.; Richardson, R. L. In "Oil Shale Tar Sands and Related Materials"; Stauffer, H. E., Ed.; American Chemical Society: Washington, DC, 1981; ACS Symp. Ser. No. 163; p 315.

(4) LaMar, G. N.; Horrocks, W. DeW; Holm, R. H., Jr. "NMR of Paramagnetic Molecules"; Academic Press: New York, 1973.

(5) Harris, R. K. "Nuclear Magnetic Resonance Spectroscopy"; Pitman Books Limited: London, 1983; p 207.

(6) Hirayama, M.; Honyu, Y. *Bull. Chem. Soc. Jpn.* **1973**, *46*, 2687.

(7) Levy, G. C.; Komoroski, R. A. *J. Am. Chem. Soc.* **1974**, *96*, 678.

0002-7863/84/1506-0557$01.50/0

Table I. Paramagnetic Shifts of Nitrogen-Heterocyclic Compounds

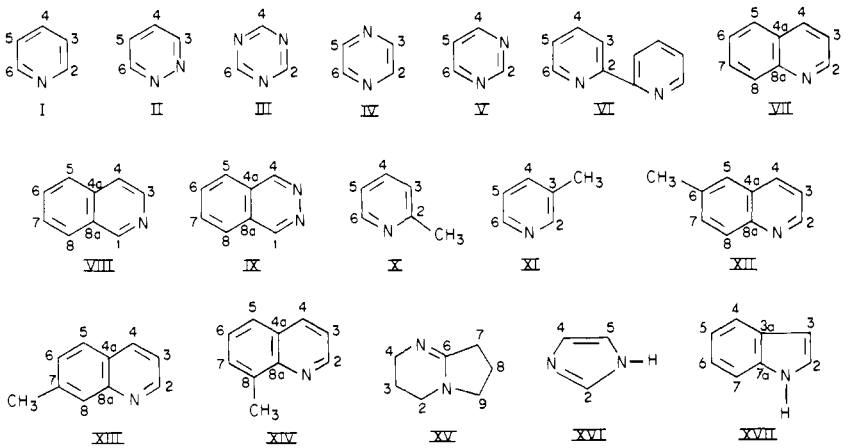

compound[a]	position	δ_o[b]	δ_o lit.	$\overline{\Delta\delta_f}^{int}$	$\overline{\Delta\delta_f}$	ref
pyridine (I)	2	150.26	150.4	2.93	6.91	15
1.75 M	3	123.85	124.1	4.15	8.13	
	4	135.94	136.1	4.87	8.85	
pyridazine (II)	3	151.81	152.8	6.93	10.91	15
1.15 M	4	126.43	127.4	9.88	13.86	
s-triazine (III)		166.33	167.50	10.95	14.93	16
0.76 M						
pyrazine (IV)		145.40	146.1	7.04	11.02	15
1.15 M						
pyrimidine (V)	2	159.58	159.7	3.57	7.55	15
1.81 M	4, 6	156.95	157.7	8.70	12.68	
	5	121.57	122.3	10.18	14.16	
pyrimidine (V)	2	159.58	159.7	3.67	7.65	15
1.16 M	4, 6	157.05	157.7	9.21	13.19	
	5	121.62	122.3	11.07	15.05	
pyrimidine (V)	2	159.58	159.7	3.44	7.42	15
0.64 M	4, 6	156.77	157.7	10.01	13.99	
	5	121.38	122.3	11.81	15.79	
2,2′-dipyridyl (VI)	2	156.56	155.25	−1.20	2.78	16
0.59 M	3	123.75	124.20	4.39	8.37	
	4	136.85	137.25	4.31	8.29	
	5	121.30	120.40	0.49	4.47	
	6	149.36	149.20	2.90	6.88	
quinoline (VII)	2	150.40	150.3	3.27	7.25	17
1.24 M	3	121.13	121.0	4.53	8.51	
	4	135.79	136.0	5.58	9.56	
	4a	128.51	128.3	−0.90	3.08	
	5	127.88	127.7	4.06	8.04	
	6	126.61	126.5	2.74	6.72	
	7	129.39	129.4	2.54	6.52	
	8	130.16	129.4	0.51	4.49	
	8a	148.90	148.3	−0.89	3.09	
isoquinoline (VIII)	1	125.83	125.5	3.86	7.84	17
1.37 M	3	143.46	143.1	2.67	6.65	
	4	120.60	120.4	4.02	8.00	
	4a	136.09	135.7	−1.02	2.96	
	5	126.76	126.5	4.26	8.24	
	6	130.45	130.3	3.63	7.61	
	7	127.40	127.2	3.66	7.64	
	8	127.88	127.5	4.21	8.19	
	8a	129.05	129.8	−0.89	3.09	
quinazoline (IX)	2	160.02	160.50	12.23	16.21	16
0.62 M	4	155.70	155.70	2.82	6.80	
	4a	125.41	125.20	−0.32	3.66	
	5	127.20	127.40	8.94	12.92	
	6	127.74	127.95	5.93	9.91	
	7	133.80	134.15	5.53	9.51	
	8	129.10	128.55	2.25	6.23	
	8a	150.56	150.15	−0.82	3.16	
2-picoline (X)	2	158.66	158.70	−1.14	2.84	16
2.04 M	3	123.27	123.20	2.86	6.84	
	4	136.18	136.10	3.97	7.95	
	5	120.79	120.80	3.40	7.38	
	6	149.44	149.50	2.13	6.11	
	Me	24.38	25.10	2.45	6.43	
3-picoline (XI)	2	150.64	150.06	1.86	5.84	16
1.27 M	3	132.54	132.84	−1.04	2.94	
	4	135.93	136.15	4.04	8.02	
	5	122.97	122.93	3.61	7.59	
	6	147.30	146.73	2.47	6.45	
	Me	18.41	18.34	4.66	8.64	
6-methylquinoline (XII)	2	149.63	149.5	2.75	6.73	17
1.41 M	3	121.18	121.0	3.98	7.96	
	4	135.35	135.3	4.49	8.47	
	4a	128.61	128.3	−1.31	2.67	
	5	126.81	126.5	2.64	6.62	
	6	136.33	136.3	−1.66	2.32	
	7	131.81	131.7	1.60	5.58	
	8	129.72	129.1	0.41	4.39	
	8a	147.44	146.9	−0.94	3.04	
	Me	21.56		3.55	7.53	
7-methylquinoline (XIII)	2	150.29	150.4	2.67	6.65	17
1.16 M	3	120.33	120.3	3.76	7.74	
	4	135.40	135.7	4.64	8.62	
	4a	126.59	126.5	−0.92	3.06	
	5	127.54	127.4	3.25	7.23	
	6	128.79	128.5	1.78	5.76	
	7	139.30	139.7	−1.37	2.61	
	8	129.16	128.8	−0.25	3.73	
	8a	149.12	148.6	−1.09	2.89	
	Me	21.82		2.97	6.95	
8-methylquinoline (XIV)	2	149.25	149.2	3.06	7.04	17
1.21 M	3	120.85	120.8	4.35	8.33	
	4	136.07	136.2	5.09	9.07	
	4a	128.51	128.2	−1.07	2.91	
	5	125.94	125.9	3.43	7.41	
	6	126.39	126.3	2.19	6.17	
	7	129.64	129.6	1.63	5.61	
	8	137.77	137.1	−1.39	2.59	
	8a	147.94	147.4	−1.07	2.91	
	Me	18.14		1.14	5.12	
1,5-Diazabicyclo-	2	43.31		3.59	7.57	
[4.3.0]nonene-5 (XV)	3	21.31		1.53	5.51	
0.57 M	4	43.82		0.89	4.87	
	6	158.90		−1.52	2.46	
	7	30.84		1.56	5.54	
	8	19.92		2.74	6.72	
	9	51.51		4.06	8.04	
imidazole (XVI)	2	135.98	135.7	4.77	8.75	15
2.47 M	4	122.25	121.8	3.28	7.26	
	5	122.25	121.8	3.28	7.26	

Table I (*Continued*)

compound[a]	position	δ_o[b]	δ_o lit.	$\overline{\Delta\delta_f}^{int}$	$\overline{\Delta\delta_f}$	ref
indole (XVII)	2	124.04	125.2	15.99	19.97	15
0.47 M	3	102.93	102.6	12.76	16.74	
	3a	128.29	128.8	9.25	13.23	
	4	121.03	121.3	1.98	5.96	
	5	122.24	122.3	0.36	4.34	
	6	120.11	120.3	0.63	4.61	
	7	111.13	111.8	13.53	17.51	
	7a	136.42	136.1	5.66	9.64	
indole (XVII)	2	124.86	125.2	9.43	13.41	15
1.23 M	3	102.73	102.6	8.62	12.60	
	3a	128.17	128.8	6.21	10.19	
	4	120.99	121.3	1.54	5.52	
	5	122.20	122.3	0.55	4.53	
	6	120.11	120.3	0.59	4.57	
	7	111.68	111.8	8.30	12.28	
	7a	136.12	136.1	3.84	7.82	
indole (XVII)	2	124.43	125.2	7.87	11.85	
2.93 M	3	102.40	102.6	6.64	10.62	
	3a	127.98	128.8	3.99	7.97	
	4	120.94	121.3	1.27	5.25	
	5	122.10	122.3	0.71	4.69	
	6	120.06	120.3	0.61	4.59	
	7	111.37	111.8	6.20	10.18	
	7a	135.89	136.1	2.71	6.69	

[a] Molarity in CCl_4. All measurements were made at room temperature (25 °C). [b] Chemical shifts were measured relative to internal cyclohexane and converted to Me_4Si by adding 27.00 ppm as described in ref 1.

tween the indole and Tempo are obtained.

Experimental Section

Tempo and all of the chemicals were purchased from Aldrich and Eastman Kodak Co. and were used directly without further purification. The samples were dissolved in either CCl_4 or $CDCl_3$ and degassed by using freeze–thaw methods.

The paramagnetic induced carbon-13 chemical shifts were measured as described earlier.[1] Spectra at 75.5 MHz for the ^{13}C nucleus with a proton-decoupling frequency of 300.2 MHz were obtained on a Varian SC-300 superconducting spectrometer. Assignments of the compounds were already known in the literature, except for 1,5-diazabicyclo-[4.3.0]nonene-5. Selective decoupling methods were used to make these assignments.

Carbon-13 spin–lattice relaxation times (T_1's) were obtained at 30 °C from normal 180–τ–90 inversion recovery FT-NMR experiments. For each sample, 10 to 15 different τ values were selected. Reproducibility of T_1 values was better than ±10% except for nonprotonated carbons in pure compounds where it was not feasible to use sufficiently long pulse delay times to achieve this level of accuracy. On the basis of initial estimates of T_1, a pulse delay of 3–5 T_1's was selected. Since only the difference of the reciprocals of T_1 were needed, the absolute errors in the very small relaxation rates of the nonprotonated carbons were no greater than those for the much larger relaxation rates of the protonated carbons.

The computer-fitting technique of Mayne et al.[8] was used to calculate T_1 from the following equation

$$S(t) = S(\infty) + [S(0) - S(\infty)] \exp(-t/T_1)$$

where $S(0) = -\alpha S(\infty)$ and the fitting parameter becomes T_1, α, and $S(\infty)$. This program also calculates the errors in these parameters from the scatter in the data.

Results and Discussion

A. Paramagnetic Induced Carbon-13 Chemical Shifts. The measured and corrected paramagnetic shifts of 17 nitrogen heterocyclic compounds dissolved in CCl_4 are listed in Table I. In samples containing different Tempo concentrations ranging from 0.1 to 1.0 M, the shifts were measured relative to an internal cyclohexane reference. Plots of the resonance frequencies vs. the concentration of Tempo were found to be linear, and a linear regression analysis of these data provides the molar free radical induced shift, $\overline{\Delta\delta_f}^{int}$, relative to the internal reference.[1]

In order to obtain the paramagnetic shift, both internal and external references were used to determine $\overline{\Delta\delta_f}^{ref}$. This shift results from changes in the bulk magnetic susceptibility associated with the free radical, $\overline{\Delta\delta_f}^{s}$, and the contact or pseudocontact interactions of Tempo with the reference compound, $\overline{\Delta\delta_f}^{m}$. The relation between these shifts is given as follows:

$$\overline{\Delta\delta_f}^{ref} = \overline{\Delta\delta_f}^{s} + \overline{\Delta\delta_f}^{m}$$

The paramagnetic shift is the sum of $\overline{\Delta\delta_f}^{int}$ and $\overline{\Delta\delta_f}^{m}$

$$\overline{\Delta\delta_f} = \overline{\Delta\delta_f}^{int} + \overline{\Delta\delta_f}^{m}$$

We measured $\overline{\Delta\delta_f}^{s}$ to be 2.88 ± 0.03 ppm using the spinning sideband method of Malinowski and Pierpaoli.[9] The average value of $\overline{\Delta\delta_f}^{ref}$ = 6.86 ± 0.10 ppm in these heterocyclic compounds is only slightly smaller than and within experimental error of the previous value of $\overline{\Delta\delta_f}^{ref}$ = 6.94 ± 0.10 ppm obtained for the aromatic hydrocarbons. With use of these values for $\overline{\Delta\delta_f}^{s}$ and $\overline{\Delta\delta_f}^{ref}$, a value of $\overline{\Delta\delta_f}^{m}$ = 3.98 ppm was obtained and used in this paper.

Systematic paramagnetic effects can be readily observed in the data given in Table I. It is noted that all nitrogen heterocycles have greater paramagnetic shifts than those observed in the corresponding aromatic compounds [e.g., pyridine 6.91, 8.13, 8.83, is compared with benzene 5.64], indicating either that there is a greater affinity between the nitrogen heterocycles and the Tempo or that the interaction is magnified in some other way by the nitrogen heterocycles. The trend in $\overline{\Delta\delta_f}$ for pyridine of para > meta > ortho indicates that the nitrogens in Tempo and pyridine tend to orient in opposite directions from one another in the collision complex, and thus the NO group containing the free electron in Tempo would be closer to the para position to give larger contact and pseudocontact shifts. Draney and Kingsbury[10] also obtained similar results using the DTBN free radical shown as follows:

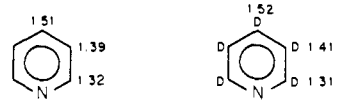

Presumably, electrostatic repulsion between the lone-pair electron of the nitrogen atom and the unpaired electron of the Tempo could account for the effect. In other nonprotonated nitrogen heterocycles the carbon position adjacent to nitrogen atoms also has the smallest $\overline{\Delta\delta_f}$ value. The data on pyridine, pyridazine, pyrazine, and *s*-triazine show that $\overline{\Delta\delta_f}$ increases in an additive manner with the number of nitrogen atoms in the nitrogen heterocyclic ring (see Table II in the regression parameters).

The linear equation is given by

$$\overline{\Delta\delta_f} = \overline{\Delta\delta_f}^{0} + \sum_{l} n_l \overline{\Delta\delta_f}(l) \qquad (1)$$

where n_o, n_m, and n_p are the numbers of nitrogen atoms ortho, meta, and para to the shifted carbons, respectively, and $\overline{\Delta\delta_f}(0)$, $\overline{\Delta\delta_f}(m)$, $\overline{\Delta\delta_f}(p)$ are the contributions of those positions to the corrected induced shift $\overline{\Delta\delta_f}$. The constant term $\overline{\Delta\delta_f}^{0}$ = 3.7 obtained in this analysis is within experimental error of the $\overline{\Delta\delta_f}^{m}$ = 3.98 obtained above for the effect of Tempo on the reference compound,

(8) Mayne, C. L.; Alderman, D. W.; Grant, D. M. *J. Chem. Phys.* **1975**, *63*, 2514.

(9) Malinowski, E. R.; Pierpaoli, A. R. *J. Magn. Reson.* **1969**, *1*, 509. Malinowski, E. R.; Weiner, P. H. *J. Am. Chem. Soc.* **1970**, *92*, 4193. See also ref 1.

(10) Draney, D.; Kingsbury, C. A. *J. Am. Chem. Soc.* **1981**, *103*, 1041.

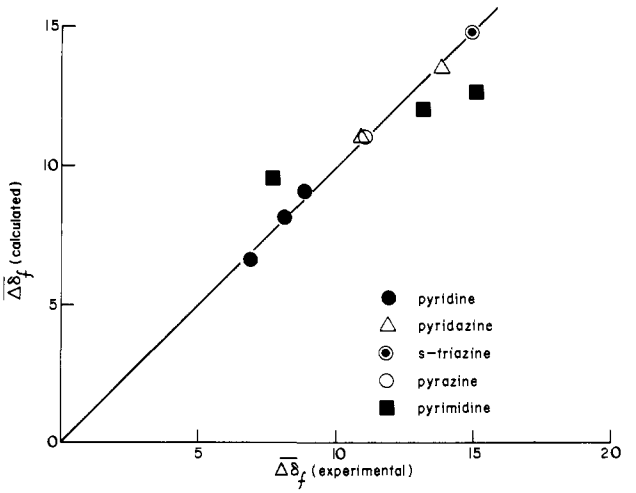

Figure 1. Correlation between calculated and experimental $\overline{\Delta\delta}_f$ for simple nitrogen heterocycles. Only data for pyrimidine show significant deviations from the linear relationship given by eq 1.

cyclohexane. The $\overline{\Delta\delta}_f(0) = 2.9$, $\overline{\Delta\delta}_f(m) = 4.5$, and $\overline{\Delta\delta}_f(p) = 5.4$ correspond closely with the $\overline{\Delta\delta}_f^{int}$ of pyridine. These results provide an insight into the contributions affecting the induced shift $\overline{\Delta\delta}_f$. The overall shift may be separated into two parts, one part arising from a general contribution that is the same for all carbons in the compound as well as for the reference carbon. The second part depends upon the relative position of the shifted carbon in the complexed heterocycle and the free electron in the Tempo radical.

Deviations from a linear relationship were found for pyrimidine as shown in Figure 1. The observed $\overline{\Delta\delta}_f$ of carbon 2 is less than the predicted value, while for carbons 4, 6, and 5 the shifts are larger than the predicted values. The exact cause of these deviations is not known, but it probably reflects a breakdown in the weak interaction assumption that is required for a linear response function. Pyrimidine, among the heterocycles included in this study, has been shown to deviate most[11] from other simple correlative relationships. Since interactions between pyrimidine and Tempo appear to be stronger, it is not surprising that the paramagnetic shifts in pyrimidine exhibit a larger concentration dependence than in the other nitrogen heterocycles. The $\overline{\Delta\delta}_f$ of carbons 4 and 5 increases with decreasing concentration of pyrimidine in accordance with the following equations:

$$\Delta\delta_f(5) = 16.67 - 1.392C \qquad R = 0.9999$$

$$\Delta\delta_f(4,6) = 14.62 - 1.106C \qquad R = 0.9817$$

where C is the concentration of pyrimidine. Other nitrogen heterocycles exhibit smaller concentration dependence.

The $\overline{\Delta\delta}_f$ values in nitrogen heterocycles, as with fused aromatic hydrocarbons, increase with the number of rings. Thus quinoline, isoquinoline, and quinazoline have larger shifts than pyridine. When methyl groups are present in the heterocycles, the shifts decrease due presumably to the methyl groups sterically hindering the complex formation. It is interesting that there exist a series of linear relationships between the $\overline{\Delta\delta}_f$ of the 2, 3, 4 positions of pyridine and the $\overline{\Delta\delta}_f$ of the corresponding 2, 3, 4 positions of quinoline. When the $\overline{\Delta\delta}_f$ of pyridine is used as X and the $\overline{\Delta\delta}_f$ of quinolines is used as Y the LRA equations are as follows:

quinoline	$Y = 1.064X - 0.027$	$R = 0.9996$
6-methylquinoline	$Y = 0.967X + 0.014$	$R = 0.9998$
7-methylquinoline	$Y = 0.965X - 0.009$	$R = 0.9998$
8-methylquinoline	$Y = 1.024X - 0.006$	$R = 0.9999$

(11) Pugmire, R. J.; Grant, D. M. *J. Am. Chem. Soc.* **1968**, *80*, 679.

Table II. Multiple Stepwise Linear Regression Analysis of the Paramagnetic Shifts in Nitrogen Heterocycles

	six heterocycles[a]		four heterocycles[b]	
multiple correl coeff	0.9961		0.9974	
standard error of estimate	±0.4 ppm		±0.3 ppm	
constant term, $\overline{\Delta\delta}_f$	3.9 ± 0.3 ppm		3.7 ± 0.3 ppm	
parameter	value	F value to remove	value	F value to remove
$\overline{\Delta\delta}_f(o)_N$	3.0 ± 0.2	196	2.9 ± 0.2	268
$\overline{\Delta\delta}_f(m)_N$	4.2 ± 0.3	229	4.5 ± 0.3	260
$\overline{\Delta\delta}_f(p)_N$	5.2 ± 0.3	351	5.4 ± 0.3	434
$\overline{\Delta\delta}_f(\alpha)_c$	−4.6 ± 0.3	179		
$\overline{\Delta\delta}_f(o)_c$	−1.1 ± 0.3	4		
$\overline{\Delta\delta}_f(m)_c$	−0.8 ± 0.3	7		
$\overline{\Delta\delta}_f(p)_c$	−0.6 ± 0.3	3		

[a] Data fitted from the experimental results of pyridine, pyridazine, *s*-triazine, pyrazine, 2-picoline, and 3-picoline. [b] The two picolines were omitted from the list in footnote *a*.

The slopes of these equations quantitatively reflect their relative interaction between Tempo and the substrate. The picolines also exhibit such linear relationships with substituent parameters. A more extensive seven parameter[12] MSLRA correlates both the nitrogen positions and the effect of methyl substituents in the picolines.

$$\overline{\Delta\delta}_f = \overline{\Delta\delta}_f^0 + \sum_l n_l\overline{\Delta\delta}_f(l) + \sum_k c_k\overline{\Delta\delta}_f(k) \qquad (2)$$

where n_o, n_m, n_p, c_o, c_m, and c_p are respectively the number of nitrogen and methyl carbons ortho, meta, and para to the carbon of concern and c_α is the ring carbon to which the methyl group is bonded. These results, given in Table II, exhibit within experimental errors the same nitrogen positional effects as found for the non-methylated heterocycles. The carbon positional parameters reflect an attenuation of the interaction with the free radical as all the substituent parameters have the opposite sign. In further support of a steric inhibition model, the methyl substituent values decrease with the distance between the carbon affected and the methyl group. The simple explanation of increasing r_{eN} due to steric considerations is sufficient to explain both the shift direction and the respective magnitudes of the methyl parameters.

Unlike the six-membered heterocycles, imidazole and indole have a hydrogen attached to the nitrogen atom, and this proton may hydrogen bond with the nitroxyl group of Tempo thereby increasing the interaction in the neighborhood of the N–H group. For example, the ortho position between the two nitrogen atoms of imidazole actually has a larger $\overline{\Delta\delta}_f$ than the remaining carbon positions unlike the pyrimidine results. Position 4 and 5 have the same value due to rapid tautomeric averaging as follows:

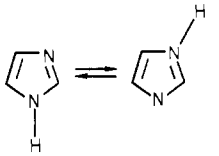

Indole exhibits very large shifts in the 2, 3, 3a, 7a, 7 positions, and these shifts are strongly dependent on the concentration of the indole. This phenomenon may be due to the competition of complexation between Tempo and either indole or CCl_4. Preliminary experiments on 1,5-diazabicyclo[4.3.0]nonene-5 show that large shifts appear at position 2, 9 indicating that a stronger interaction is found in the neighborhood of the bridgehead nitrogen at position 1. It is generally accepted that bridgehead nitrogens carry a higher differential positive charge than ring nitrogens

(12) MSLRA programmed by D. K. Dalling following an algorithm detailed by Draper and Smith: Draper, N. R.; Smith, H. "Applied Regression Analysis", 2nd ed.; Wiley: New York, 1981.

Table III. Spin-Lattice Relaxation Data

compound[a]	C position	no Tempo T_1[b]	intermediate Tempo concn of Tempo, M	intermediate Tempo T_1[b]	higher Tempo concn of Tempo, M	higher Tempo T_1[b]	R_{exptl}[e]
nephthalene	1	10.8 ± 0.8	0.045	4.7 ± 0.5	0.110	2.1 ± 0.2	3.49
0.96 M	2	9.8 ± 0.4		3.7 ± 0.2		1.9 ± 0.1	3.92
	9	47.0 ± 8.0		6.0 ± 1.0		2.8 ± 0.3	2.99
pyridine	2	15.0 ± 1.0	0.071	3.3 ± 0.2	0.122	2.4 ± 0.2	2.89
1.29 M	3	17.0 ± 1.0		3.0 ± 0.1		2.0 ± 0.1	3.55
	4	13.0 ± 1.0		2.8 ± 0.2		2.1 ± 0.1	3.23
pyridazine	3	17.0 ± 2.0	0.056	3.3 ± 0.2	0.099	1.6 ± 0.1	5.49
1.30 M	4	15.0 ± 0.8		2.7 ± 0.2		1.3 ± 0.1	6.89
s-triazine		13.0 ± 1.0	0.068	2.2 ± 0.2	0.164	1.0 ± 0.1	5.68
1.21 M							
pyrazine		14.4 ± 0.6	0.095	2.2 ± 0.2	0.164	1.3 ± 0.1	4.14
1.66 M							
pyrimidine	2	11.3 ± 0.8	0.098	2.2 ± 0.2	0.136	2.0 ± 0.2	3.11
1.00 M	4, 6	11.2 ± 0.6		1.8 ± 0.2		1.6 ± 0.2	4.09
	5	10.0 ± 1.0		1.6 ± 0.2		1.4 ± 0.1	4.83
quinazoline	2	6.0 ± 0.3	0.071	1.6 ± 0.1	0.151	1.0 ± 0.1	5.55
0.71 M	4	4.6 ± 0.2		2.1 ± 0.2		1.3 ± 0.1	3.78
	9	46.0 ± 8.0		3.7 ± 0.4		1.5 ± 0.2	4.18
	7	4.8 ± 0.3		1.8 ± 0.1		1.0 ± 0.1	5.37
	8	6.4 ± 0.3		2.1 ± 0.2		1.2 ± 0.1	4.57
	6	4.6 ± 0.2		1.8 ± 0.2		0.9 ± 0.1	5.98
	5	6.3 ± 0.4		1.9 ± 0.2		0.9 ± 0.1	5.97
	10	46.0 ± 12.0		2.9 ± 0.3		1.4 ± 0.1	4.50
indole	2	6.4 ± 0.2	0.050	1.0 ± 0.1	0.092	0.6 ± 0.1	16.79
0.951 M	3	7.1 ± 0.4		2.0 ± 0.1		1.2 ± 0.1	7.28
	4	7.2 ± 0.4		2.4 ± 0.2		1.6 ± 0.1	5.12
	5	6.6 ± 0.3		2.0 ± 0.1		1.3 ± 0.1	6.85
	6	6.6 ± 0.3		2.4 ± 0.1		1.4 ± 0.1	5.95
	7	7.4 ± 0.2		1.3 ± 0.1		0.7 ± 0.1	14.72
	3a	61.0 ± 9.0		2.5 ± 0.1		1.5 ± 0.2	6.76
	7a	80.0 ± 30.0		1.3 ± 0.1		0.5 ± 1.0	19.86
indole	2	4.9 ± 0.3	0.052	1.1 ± 0.1	0.101	0.6 ± 0.1	14.16
1.737 M	3	5.7 ± 0.3		1.8 ± 0.1		1.2 ± 0.1	6.64
	4	5.6 ± 0.2		2.1 ± 0.1		1.4 ± 0.1	5.15
	5	5.5 ± 0.2		1.8 ± 0.2		1.2 ± 0.1	6.34
	6	4.9 ± 0.2		1.8 ± 0.1		1.2 ± 0.1	6.04
	7	5.1 ± 0.3		1.2 ± 0.1		0.8 ± 0.1	10.81
	3a	42.0 ± 7.0		2.4 ± 0.2		1.2 ± 0.1	7.72
	7a	52.0 ± 12.0		1.1 ± 0.1		0.6 ± 0.1	15.94

[a] Molarity in $CDCl_3$. All data were taken at room temperature (25 °C). [b] Seconds.

providing more favorable electrostatic interactions with the NO group in Tempo for $N-1$ vs. $N-5$.

B. Spin–Lattice Relaxation Measurements. The spin–lattice relaxation times of eight compounds dissolved in $CDCl_3$ are listed in Table III. For concentration i the observed relaxation rate, $R_{1,i}^{obsd}$, is given as

$$R_{1,i}^{obsd} = R_1^{dia} + R_{1,i}^{e} \quad (3)$$

where R_1^{dia} is equal to $R_{1,0}^{obsd}$ of the pure compound. Therefore, $R_{1,i}^{e}$ may be obtained as follows

$$R_{1,i}^{e} = R_{1,i}^{obsd} - R_{1,0}^{obsd} \quad (4)$$

We observed that $R_{1,i}^{e}$ are linearly dependent on the concentration of Tempo, and LRA methods may be used to calculate the molar electron nuclear relaxation rate, $\bar{R}_1^{e}$, induced by the Tempo from the slope of the plots. These are given in Table III.

In naphthalene, the three $\bar{R}_{exptl}^{e}$ exhibit only minor differences. The order at positions $2 > 1 > 9$ parallels the pagamagnetic shift data. Pyridine also has similar $\bar{R}_1^{e}$ values with a positional order of $3, 4 > 2$. These also parallel the paramagnetic shift data. The relatively small $\bar{R}_{exptl}^{e}$ values and minor differences between different carbon atoms indicate that the interaction between pyridine and Tempo is relatively uniform, resulting from a weak collision-type complexation process. If the intermolecular nitrogen atoms repel one another during the collision complexation process, slight differences in both R_1^{e} and $\overline{\Delta\delta_f}$ will be noticed as a function of position similar to the case of benzonitrile and $Cr(acac)_3$ as discussed by Levy and Komoroski.[7] In the other nitrogen heterocycles, $\bar{R}_1^{e}$ values also follow the same order as the corresponding shift data. The $\bar{R}_1^{e}$ of pyridazine, *s*-triazine, pyrazine, and pyrimidine are greater than that of pyridine, indicating that the interaction becomes stronger due to increasing the number of molecular nitrogens. In quinazoline, larger values of $\bar{R}_1^{e}$ appear also at position 2 in addition to positions 5, 6, and 7, and the $\bar{R}_1^{e}$ for 4, 8, 9, and 10 are relatively small. This observation becomes important in light of the discrepancy between the shift of carbon 2 of pyrimidine which is small and the shift of carbon 2 of quinazoline which is extremely large. The agreement of the relaxation rate data with the corresponding shift data suggests that carbon 2 of quinazoline is closer to the free electron center in the Tempo molecule.

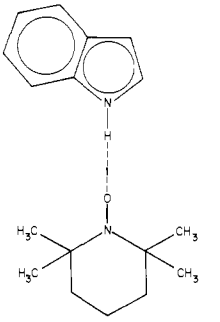

Figure 2. Static model of indole–Tempo hydrogen bond complex (the bond length of indole is assumed to be 1.4 Å).

The relaxation data for indole may be explained[7] with a hydrogen-bond complex of indole with Tempo (structure given in

Table IV. Comparison of Experimental and Calculated Molar Electron Nuclear Relaxation Rates, $\overline{R^e}$

compound	carbon	concn of Tempo, M	R_1^e- (exptl)	R_1^e- (calcd)	concn of Tempo, M	R_1^e exptl	R_1^e calcd	$\overline{R^e}$ exptl	$\overline{R^e}$ calcd	$(r_{2x}/r_{jx})^6$
indole	2	0.050	0.87	0.87	0.092	1.54	1.58	16.76	17.18	1 (*standard)
0.951 M	3		0.37	0.37		0.67	0.69	7.29	7.47	0.203
	4		0.27	0.29		0.47	0.53	5.12	5.71	0.058
	5		0.34	0.28		0.63	0.51	6.85	5.58	0.048
	6		0.26	0.32		0.55	0.59	5.95	6.40	0.115
	7		0.64	0.63		1.36	1.15	14.72	12.44	0.611
	3a		0.37	0.37		0.62	0.69	6.76	7.47	0.203
	7a		0.77	0.86		1.84	1.58	19.86	17.18	1
indole	2	0.052	0.73	0.74	0.101	1.43	1.40	14.16	14.16	1 (*standard)
1.737 M	3		0.38	0.36		0.67	0.69	6.64	6.86	0.203
	4		0.28	0.29		0.52	0.56	5.15	5.53	0.058
	5		0.37	0.28		0.64	0.55	6.34	5.44	0.048
	6		0.33	0.31		0.61	0.61	6.04	6.05	0.115
	7		0.66	0.55		1.09	1.07	10.81	10.60	0.611
	3a		0.39	0.36		0.78	0.69	7.72	6.86	0.203
	7a		0.86	0.74		1.61	1.43	15.94	14.16	1

Figure 2). Assuming the electron relaxation mechanism is dominated completely by the nuclear dipole–dipole interaction, a sixth power distance dependence is expected for the relaxation. It is further assumed that the relaxation arises from a combination of a general term, $R_1^e(f)$, affecting all carbons equally and arising from free Tempo in the solution and a structurally specific H-bond term, $R_1^e(c)$. In the limit of fast exchange between the complexed and uncomplexed species, then

$$R_1^e = x_f R_1^e(f) + x_c R_1^e(c) \tag{5}$$

where x_f and x_c are the mole fractions of the indole in the free or complexed state, respectively. In low Tempo concentrations, x_c is small and x_f is approximately equal to 1. Therefore, the approximate ratio between $R_{1i}^e(c)$ of carbon i and $R_{1s}^e(c)$ of reference carbon atom s is given by

$$\frac{R_{1i}^e - R_1^e(f)}{R_{1s}^e - R_1^e(f)} = \frac{R_{1i}^e(c)}{R_{1s}^e(c)} \tag{6}$$

Assuming $R_1^e(f)$ is the same for all carbon nuclei in indole, then the ratio $R_{1i}^e(c)/R_{1s}^e(c)$ will be equal to $(r_{sx}/r_{ix})^6$ for the dipole–dipole relaxation mechanism. Here r_{ix} is the distance between carbon i and the paramagnetic center, x, which can be calculated in terms of the distance (r_0) between the NH and the paramagnetic center. In previous work,[7] a R_1^e value of a remote carbon was used for $R_1^e(f)$ and r_0 determined from the best fit of the experimental data. A slightly more sophisticated model for fitting R_1^e is used by taking both $R_1^e(f)$ and r_0 to be fitting parameters. Using a series of different $R_1^e(f)$ and r_0 values, one may calculate a two-dimension surface for the standard deviation of the fit from the following:

$$\sigma = \sum_i \left\{ \frac{[R_{1i}^e - R_1^e(f)]}{[R_{1s}^e - R_1^e(f)]} - \left(\frac{r_{sx}}{r_{ix}}\right)^6 \right\}^2 \tag{7}$$

The minimum in this surface appears for r_0 in the range 3.0 to 3.5 Å and for $R_1^e(f) \approx 5$. Thus, the r_0 value is very close to the value of the hydrogen bond distance cited in the literature.[13] The bond lengths of NH and NO are approximately 1.0 Å, and the H–O distance is about 2.0 Å. Using these values along with an r_0 value of 3.0–3.5 Å places the unpaired electron of the Tempo somewhere between the terminal oxygen and the middle of the N–O bond. Thus a rather simple model provides a consistent and logical interpretation of the relaxation process. The value of 5 for $R_1^e(f)$ is consistent with the corresponding values observed for remote carbons 4, 5, and 6 in indole.

The relaxation data can be explained quantitatively with simple mass action principles. Consider,

$$S + F \overset{K}{\rightleftharpoons} C$$

$$K = \frac{c}{(S_0 - c)(F_0 - c)}$$

$$K[S_0F_0 - c(S_0 + F_0) + c^2] = c$$

where S_0 and F_0 are the initial or total concentrations of indole and free radical, respectively, and c is the concentration of the complexed molecule. For low free radical concentrations, both F_0 and c are small, and the c^2 term can be neglected. Therefore,

$$c \approx \frac{KS_0F_0}{1 + K(S_0 + F_0)} \qquad x_c \approx \frac{c}{S_0} = \frac{KF_0}{1 + K(F_0 + S_0)} \tag{8}$$

$$x_f = \frac{S}{S_0} \approx 1$$

Equations 5 and 8 combine for two different indole concentrations to yield:

$$\frac{(R_1^e)_{1i} - R_1^e(f)}{(R_1^e)_{2i} - R_1^e(f)} = \frac{x_{c1}}{x_{c2}} = \frac{F_{01}[1 + K(S_{02} + F_{02})]}{F_{02}[1 + K(S_{01} + F_{01})]} \tag{9}$$

The data for carbon 2 with a value of $R_1^e(f) = 5$ may be used in eq 9 to give a value of $K = 0.89$ M^{-1}. This value is comparable with results of Sysoeva et al.,[14] using a different theory for CH_3OH ($K = 3$ M^{-1}), C_2H_5OH ($K = 0.7$ M^{-1}), and $CHCl_3$ ($K = 0.6$ M^{-1}).

For $K = 0.89$ M^{-1}, the mole fractions of the complexed species are as follows:

concn of indole, M	concn of Tempo, M	x_c
0.951	0.050	0.0235
0.951	0.092	0.0425
1.737	0.052	0.0179
1.737	0.101	0.0341

Using these results for x_c one may calculate $R_1^e = 1.58$ and 1.40 with eq 5 and 8 in good agreement with the experimental values 1.54 and 1.43 for carbon 2 concentrations of indole 0.951 and 1.737 M, respectively.

These calculated values for $R_{1,i}^e$ give a value for $\bar{R}_1^e$ of carbon 2 of 0.951 M indole of 17.18 (expt. value 16.76) from which the

(13) Coulson, C. A. "Valence", 2nd Ed.; Oxford University Press: London, 1961. Hamilton, W. C.; Ibers, J. A. "Hydrogen Bonding in Solids; Methods of Molecular Structure Determination"; W. A. Benjamin: New York, 1968.

(14) Sysoeva, N. A.; Karmilov, Y.; Buchachenko, A. L. *Chem. Phys.* **1975**, *7*, 123; *Chem. Phys.* **1976**, *15*, 313, 321.

(15) Stothers, J. B. "Carbon-13 NMR Spectroscopy"; Academic Press: New York, 1972.

(16) Breitmaier, E.; Haas, G.; Voelter, W. "Atlas of Carbon-13 NMR Data"; Heyden: New York, 1979.

(17) Su, J.-A.; Siew, E.; Brown, E. V.; Smith, S. L. *Org. Magn. Reson.* **1977**, *10*, 122.

corresponding values of other carbons can be calculated by using the equation

$$(R_1^e)_i = R_1^e(f) + \left(\frac{r_{2x}}{r_{ix}}\right)[(R_1^e)_2 - R_1^e(f)] \qquad (10)$$

The results given in Table IV indicate very good agreement between theory and experimental results. This is especially noteworthy since the competition between indole and $CDCl_3$ for Tempo has been neglected and since the electron nuclear dipole–dipole interaction has been assumed to dominate completely the relaxation in the complex.

Acknowledgment. We thank Dr. Eric Johnston, Dr. D. Dalling, and Mark S. Solum for their valuable discussions and experimental assistance. This work was supported by the Department of Energy, Division of Fossil Energy, under the Grant No. DE-FG22-80PC30226.

Registry No. Pyridine, 110-86-1; pyridazine, 289-80-5; *s*-triazine, 290-87-9; pyrazine, 290-37-9; pyrimidine, 289-95-2; 2,2′-dipyridyl, 366-18-7; quinoline, 91-22-5; isoquinoline, 119-65-3; quinazoline, 253-82-7; 2-picoline, 109-06-8; 3-picoline, 108-99-6; 6-methylquinoline, 91-62-3; 7-methylquinoline, 612-60-2; 8-methylquinoline, 611-32-5; 1,5-diazabicyclo[4.3.0]non-5-ene, 3001-72-7; imidazole, 288-32-4; indole, 120-72-9; naphthalene, 91-20-3; Tempo, 2564-83-2.

Representation of Electron Densities. 1. Sphere Fits to Total Electron Density Surfaces

Michelle M. Francl,[1a] Robert F. Hout, Jr.,[1b] and Warren J. Hehre*

Contribution from the Department of Chemistry, University of California, Irvine, California 92717. *Received April 22, 1983*

Abstract: A method is detailed enabling fits to calculated total electron densities using spheres of adjustable radii centered on the nuclear positions. Best atomic radii are obtained for a series of molecules with use of Hartree–Fock models. Minimal split-valence and polarization basis set results are compared. The dependency of atom size (in molecules) on the electronegativity of attached groups and on steric and strain conditions is examined, and a set of average radii for use in molecular models is proposed. Comparisons between calculated radii and atomic charges obtained from Mulliken population analyses suggest that the latter method generally underestimates the population of hydrogen and overestimates the population of lithium and sodium.

The size and shape of a molecule are defined by the positions of the nuclei and the spatial distribution of the electrons about them. As such, visual representations of electron distributions, i.e., *electron densities*, can be instrumental in helping in the understanding of both the structures of molecular systems and their potential reactivity. Because some electron density may be found even at very large distances from the nuclear positions, examination of the *total electron density* function itself is not revealing. More useful is a representation obtained by constructing an *electron density surface*, defined by a fixed *electron density contour*, within which the volume, surface area, various contact distances, etc., are determined and, given identical contours, may be compared for different molecules.

The determination of electron density surfaces from quantum mechanical wave functions is not yet practical for all systems of interest, e.g., large biomolecules. Still, some idea of the "electronic" size and shape of a particular species may be garnered by constructing space-filling representations with, for example, CPK models.[2] Such representations, while easily manipulated and highly portable, will not be as accurate nor as flexible as direct portrayals of the electron density as calculated from quantum mechanics. Nevertheless, in many instances models of this type may provide significant information.

In order to combine the convenience and portability of CPK-type models with the inherent accuracy and generality of quantum mechanical electron density representations, we have recently developed a technique for fitting calculated electron density surfaces to spheres centered on the nuclei.[3] In addition to the obvious convenience, i.e., portability, brought about by representing calculated electron densities by nuclear-centered spheres, definition of the set of "optimum" radii for atoms in a molecule provides a means for assessing *intramolecular* electronic effects. For example, one would expect to see the effects of substitution by electron-withdrawing and electron-donating groups manifested as the decrease or increase, respectively, of the size, i.e., radius, of the atom to which the substituent is attached. Effects on atom size could be quantified and might be related to (or even used as a measure of) substituent electronegativity. In addition, relationships between the sizes of atoms in molecules and measurable properties such as NMR chemical shifts and coupling constants might be anticipated.

The use of models in which atoms in molecules are represented as interconnecting spheres, while presumably obscuring features such as π clouds and nonbonded lone pairs, is, in fact, not without support. It has previously been noted that electron densities formed by the superposition of calculated atom densities effectively mimic actual surfaces.[4] Models constructed on this basis usually assume that the radius of a particular element is invariant, or that it can be approximated by one of a small set of fixed radii for different molecular environments.[5] The variation, or lack thereof, in atomic size as evaluated by comparing radii from sphere fits can provide some notion of the transferability of this type of data.

The partitioning of the space occupied by a molecule into spherical regions is not an unusual approach. Such schemes have been used to evaluate atomic populations. Radii for these analyses have been established in a variety of ways, e.g., using tabulated van der Waals radii[6] and the radius at which the spherically averaged density is at a minimum.[7] In the SCF-Xα-SW method[8]

(1) (a) Chevron Fellow. (b) Present address: Stuart Pharmaceutical, ICI Americas, Wilmington, DE.
(2) (a) W. L. Koltun, *Biopolymers*, **3**, 665 (1965); (b) R. B. Corey and L. Pauling, *Rev. Sci. Instrum.*, **24**, 621 (1953).
(3) R. F. Hout, Jr., and W. J. Hehre, *J. Am. Chem. Soc.*, **105**, 3728 (1983).
(4) A. T. Hagler and A. Ladiccirella, *Biopolymers*, **16**, 1167 (1967).
(5) A. Walton, "Molecular and Crystal Structure Models", John Wiley and Sons, New York, 1978.
(6) S. M. Dean and W. G. Richards, *Nature (London)*, **256**, 473 (1975).
(7) (a) S. Iwata, *Chem. Phys. Lett.*, **69**, 305 (1980); (b) K. Takano, H. Hosoya, and S. Iwata, *J. Am. Chem. Soc.*, **104**, 3998 (1982).

0002-7863/84/1506-0563$01.50/0